Infrared Physics & Technology 54 (2011) 278–282

Contents lists available at ScienceDirect

Infrared Physics & Technology

journal homepage: www.elsevier.com/locate/infrared

Colloidal quantum dot photodetectors

Gerasimos Konstantatos [a], Edward H. Sargent [b,*]

[a] ICFO-Institut de Ciencies Fotoniques, Mediterranean Technology Park, 08860 Castelldefels, Barcelona, Spain
[b] Department of Electrical and Computer Engineering, University of Toronto, 10 King's College Road, Toronto, Ontario, Canada M5S 3G4

ARTICLE INFO

Article history:
Available online 25 December 2010

Keywords:
Photodetectors
Colloidal quantum dots
Photoconductive gain
Photodiodes
Solution-processed

ABSTRACT

We review recent progress in light sensors based on solution-processed materials. Spin-coated semiconductors can readily be integrated with many substrates including as a post-process atop CMOS silicon and flexible electronics. We focus in particular on visible-, near-infrared, and short-wavelength infrared photodetectors based on size-effect-tuned semiconductor nanoparticles made using quantum-confined PbS, PbSe, Bi_2S_3, and In_2S_3. These devices have in recent years achieved room-temperature D^* values above 10^{13} Jones, while fully-depleted photodiodes based on these same materials have achieved MHz response combined with 10^{12} Jones sensitivities. We discuss the nanoparticle synthesis, the materials processing, integrability, temperature stability, physical operation, and applied performance of this class of devices.

1. Introduction

Materials that can absorb light where silicon does not are of great potential interest in photodetection and imaging. Also of interest are avenues to enhance photodetector sensitivity across all spectral regimes including the visible: strategies include top-surface detectors having 100%-fill-factor; and means of signal amplification within the photodetector itself, including carrier multiplication and photoconductive gain [1,2].

These considerations motivate intense interest in new materials and structures that expand the spectrum of absorption; minimize the thickness of semiconductor needed to absorb light completely; and amplify signal. Ideally, these materials should be integrable with silicon electronics [3], or with flexible substrates such as those based on organic and polymer materials [4]. Ink-jet printing, solution-casting, low-temperature evaporation, and layer-by-layer techniques are thus very attractive alternatives to high-temperature epitaxy [5].

Here we review recent advances in light sensing, focusing on materials compatible with low-temperature processing and large-area integration. We focus in particular on colloidal quantum dots (CQDs) [6] in which nanoscale phenomena such as quantum confinement [7] play a major role. Colloidal quantum dots are nanostructured materials synthesized and processed from solution phase. They benefit from the quantum size effect, wherein the bandgap of the material is strongly dependent on the size of the nanocrystals. Rapid advances in colloidal quantum dot synthesis and photophysics [7] have led to a high degree of control over nanoparticle size, shape, and composition [6].

The confinement of charge carriers in a colloidal quantum dot means that they occupy discrete energy levels, like the electrons in an atom. The strong confinement experienced by the charge carriers also influences the various mechanisms that are involved in charge transport in solids made from quantum dots, including delocalization [8], variable-range hopping [9], slow carrier relaxation [10], and the interactions between electrons and holes [11–15]. Multicarrier effects in nanoparticles can be exploited in photodetection applications to achieve performance enhancements via carrier multiplication. More broadly, these effects can provide optical gain for lasing, strong nonlinear interactions for optical signal processing, and the possibility of enhanced light harvesting in photovoltaics.

In this review we discuss two different types of photodetector (photodiodes and photoconductors); and summarize the performance of solution-processed photodetectors; discuss the device concepts, materials and physical phenomena that have underpinned these improvements in performance.

2. Quantitative progress in performance

We present in Table 1 progress in key figures of merit for solution-processed photodetectors devices (Refs. [16–32]). Both reports in which sensitivity is given, as well as those from which it can be inferred, are included in this table.

The results in Table 1 fall into two performance classes, one corresponding to photodiodes and the other to photoconductors. In a photodiode the electrons and holes generated by the incoming photons move to opposite electrical contacts (Fig. 1a), so the

* Corresponding author. Tel.: +1 416 946 5051; fax: +1 416 971 3020.
E-mail address: ted.sargent@utoronto.ca (E.H. Sargent).

1350-4495/$ - see front matter © 2010 Elsevier B.V. All rights reserved.
doi:10.1016/j.infrared.2010.12.029

Table 1
Progress in solution-processed photodetector performance.

Ref.	Year	λ (nm)	EQE (%)/ responsivity (A/W)	D^{*}[a] measured (Jones)	D^{*}[b] infrared (Jones)	3 dB BW (Hz)	Mechanism	Material	Features
[16]	1994	400–650	0.2 A/W		3×10^{10}	10^{3}	PD	MEH-PPV + C60, P3OT	Early organic photodiode
[17]	1996	400–650	60%				PD	MEH-PPV + CdS(Se) QDs	Early polymer-QD nanocomposite photodiode
[18]	2000	500–700	75%		10^{12}	4×10^{8}	PD	CuPC/PTCBI	Ultrafast
[19]	2005	400–700	0.2%		10^{8}	5×10^{4}	PD	CdSe QDs	Early quantum dot photodiode
[20]	2006	Vis- 1300	2700 A/W	2×10^{13}	5×10^{13}	2×10^{1}	PC	PbS QDs	Record sensitivity; pure quantum dot device
[21]	2007	Vis-850	120 A/W	5×10^{12}	3×10^{13}	2×10^{1}	PC	PbS QDs	Visible-only device using ultra – confined dots
[22]	2007	Vis-3000	4.4 A/W	3×10^{10}		10^{1}	PC	HgTe QDs	Long wavelength operation
[23]	2008	350–650	50 A/W		5×10^{12}		PC	P3HT + PCBM + CdTe QDs	Sensitive heterojunction device
[24]	2008	Vis-850	10 A/W		1.3×10^{13}	5×10^{1}	PC	PbS QDs	High uniformity device
[25]	2008	Vis-850	12 A/W	10^{12}		3×10^{1}	PC	PbS QDs	Single trap timeconstant
[26]	2008	Vis-900	20 A/W	10^{11}		2×10^{1}	PC	Bi_2S_3 Nanocrystals	Pb-free, single time constant
[27]	2008	370–395	61 A/W		1.3×10^{15}	10^{0}	PC	ZnO QDs	UV sensitivity
[28]	2009	250–930	18 A/W		1.5×10^{14}	3×10^{1}	PC	PbS QDs	Multiexciton-generation-enhanced
[29]	2009	Vis-1600	0.2 A/W	10^{12}		10^{6}	PD	PbS QDs	MHz response in fully-depleted photodiode
[30]	2009	Vis-1300	51%	2×10^{9}		2×10^{3}	PD	PbS QDs + PCBM + P3HT	Integrated into an image array
[31]	2009	Vis-1450	20%		10^{12} NIR10^{13} Vis		PD	PDDTT + PCBM	Long wavelength polymer photodetector
[32]	2009	400–600	1.5×10^{-5} A/W			10^{8}	PC	ZnO infiltrating CQD films	Ultrafast

[a] Measured D^{*} obtained from the combination of measured responsivity and measured noise current spectral density.
[b] Infrared D^{*} based on assumption that noise current spectral density is dominated by shot noise in the dark current. This provides a fundamental upper bound on the D^{*} that may actually be achieved in this device.

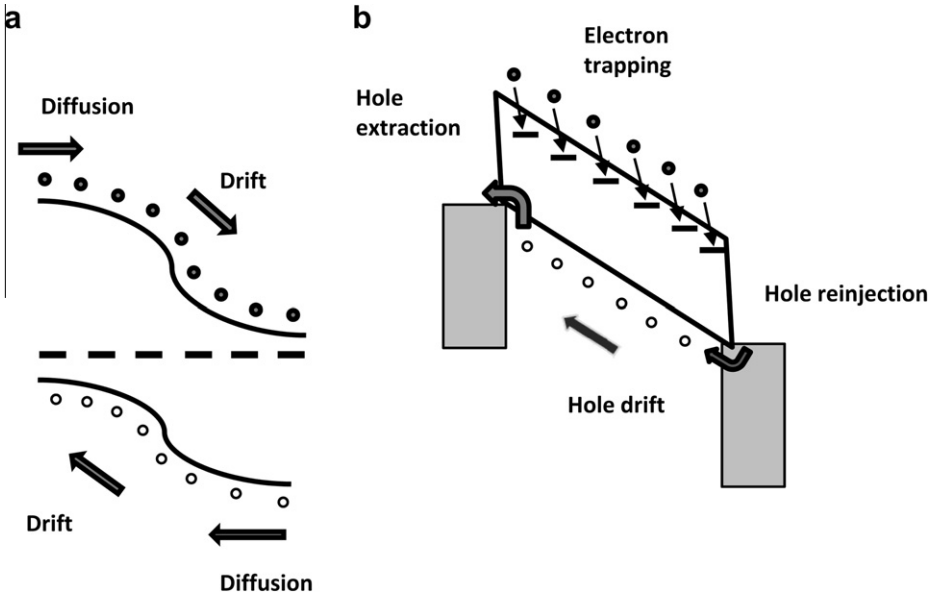

Fig. 1. Photodiodes and photoconductors: charge separation mechanisms and device structures and configurations. (a) Upon light absorption, the energy of the photon is transferred to an electron in the semiconductor, elevating it to the conduction band (upper black line) and leaving behind a hole in the valence band (lower black line). This spatial band diagram depicts the junction between a p-type (hole-rich, left side) and n-type (electron-rich, right side) semiconductor near equilibrium. In this p–n junction diode, the dashed line represents the Fermi level. Drift and diffusion of both electrons (filled circles) and holes (open circles) are exploited in photodiodes, Electron–hole pairs are separated by the action of a built-in electric field represented by the spatial bending of the bands. (b) In a photoconductor, one type of carrier is trapped while the other circulates under the influence of an electric field (electrons are trapped in this depiction). If the hole lifetime exceeds the time it takes for the hole to transit the device, then the long lifetime of the trapped electrons ensures that holes can circulate through an external circuit many times, resulting in gain.

quantum efficiency of such devices cannot be higher than 1 (unless effects such as avalanche or carrier multiplication are exploited). However, photodiodes can have fast response times, less than electron–hole recombination times, which are typically microseconds or less for the direct-gap semiconductors commonly used. Photodiodes thus populate the higher-frequency reaches of Table 1.

Photoconductors, on the other hand, are capable of high gain [33] because one type of charge carrier (say holes) is able to circulate through an external circuit many times before it recombines with its opposite carrier (say electrons), which remain trapped in the photoconductor bulk in the meantime (Fig. 1b). Table 1 lists a number of photoconductors with responsivities in the range of

100–1000 A/W, corresponding to gains of 100–1000. While these high gains increase responsivity and simplify the job of any photodetector read-out circuits, they also reduce the bandwidth because of the long circulating carrier lifetimes involved.

The performance of a photodetector can be improved, not only by maximizing its electrical response to light, but also by minimizing the noise in its electrical output, which can obscure real signals. One way to compare detector sensitivities is thus to examine the signal-to-noise level at a given illumination intensity. Or, conversely, one can examine the noise-equivalent power (NEP), which reports the optical power at which the signal-to-noise ratio (SNR) is 1 (or 0 dB). This noise level is very small, corresponding in some photodetectors to single-photon detection per integration period [34].

The normalized detectivity D^* is equal to $(A_dB)^{1/2}R/i_n$ (expressed in cm $Hz^{1/2}$/W or Jones) where A_d is the detector's active area, B is the noise measurement bandwidth, R the responsivity, and i_n the noise current. D^* is a figure of merit that seeks to normalize for variations in device area and speed of response, thus providing a metric that enables comparison among different devices [35]. Table 1 shows that the best solution-processed detectors have achieved D^* values of up to 5×10^{13}, which is comparable with the best values reported for single-crystal photodiodes. This a remarkable achievement because single-crystal photodiodes have benefited from multiple decades of engineering, including both materials purification and device structure optimization, whereas solution-processed detectors have reached similar levels of performance after just three years of development.

3. Photodiode mechanisms and performance

Photodiodes rely on the use of two media – atleast one of them a semiconductor – in which a difference in the materials' work functions produces a built-in potential. An internal field in the semiconductor depletion region near the junction propels electrons and holes in opposite directions. In the simple case of a fully-depleted device, high internal quantum efficiency is achieved if $t_{life} > t_{extract}$, where t_{life} is the lifetime of excess charge carriers, and $t_{extract} = L^2/\mu V_{bi}$ is the time taken to transport them to their respective contacts via the built-in field. In addition, L is the contact separation, μ is the mobility of the slower carrier, and V_{bi} is the built-in potential across the junction [36].

In conventional crystalline semiconductors, mobilities lie in the range 10^2 cm^2/Vs and above: charge carriers are thus readily swept a distance of 1 μm via a built-in potential of 1 V in times faster than nanoseconds. This comfortably outpaces the recombination time in both direct and indirect semiconductors. Solution-processed semiconductors have much lower mobilities – 10^{-5}–10^{-3} cm^2/Vs are typical – and thus, even for a thin depletion region 100 nm thick and a typical built-in voltage of 1 V, drift times are in the range 100 ns–10 μs. Fortunately, some of the most promising semiconductors incorporated into colloidal quantum dots used in solution-processed photodetector realization have unusually long exciton lifetimes – greater than 1 μs [37] – that have led to excellent photodiode quantum efficiencies, with even the first reports well above 50% when absorbance was high [36,38–43]. The high internal quantum efficiencies these findings entail also indicate that – when their surfaces are well-passivated using suitably-functionalized ligands – colloidal quantum dot solids achieve carrier lifetimes comparable to their exciton lifetimes: thus, well-passivated colloidal quantum dots incorporated into densely-packed solid-state films do not suffer from an excess of nonradiative recombination such as that assisted by midgap recombination centers [44]. Since the absorbance of many materials is in the 10^4–10^5 cm^{-1} range near the absorption onset, only reaching 10^6 cm^{-1} far above the bandgap, it is of interest to make devices that include light-absorption moieties as thick as micrometers. Typically, doping control in colloidal quantum dot solids has led to devices that are fully-depleted only if their thicknesses are 100–200 nm [36]. A majority of micrometer-thick devices will in this case be far from fully-depleted, demanding efficient transport through a quasi-neutral layer. In this case, the mechanism of minority carrier diffusion will be relied upon to convey carriers to the edge of the depletion region to benefit from electron–hole pair separation and extraction.

The diffusion lengths of excitons in organic semiconductors have been measured, in a wide variety of materials, to be rather short, lying in the 5–20 nm range [45]. Fortunately, in certain colloidal quantum dots solids, minority diffusion lengths in excess of 100 nm, and reaching as high as 200 nm, have been observed [29,40]. It is believed that, in these works, the use of very short, conjugated organic linkers – in this case, benzenedithiol – facilitated interdot transport, while the thiol end functional group ensured passivation. Minority electron mobilities of 10^{-3} cm^2/Vs combined with an absence of midgap traps [44] thus extended diffusion lengths into to these very attractive lengthscales for solution-cast direct-gap optoelectronic materials. There is now widespread evidence that much higher mobilities of 10^{-1} cm^2/Vs and greater may be achieved in colloidal quantum dot films [8]; once these are combined with efficient passivation and excellent film morphology, considerable further device improvements are within view.

One result in Table 1 stands out for its combination of excellent sensitivity ($D^* = 10^{12}$ Jones) and high bandwidth in the MHz range [29]. This high, directly-measured D^* is all the more remarkable for the small bandgap of the device, which provided sensitivity out to 1.6 μm. This is the wavelength of interest for night time imaging, allowing images to be collected using only the sky's own nightglow [46]. High sensitivity was achieved via the joint optimization of electron and hole transport, leading to high quantum efficiencies, as well as control over film morphology and defect passivation, which maximized the shunt resistance and minimized dark current. The MHz temporal response was achieved through the realization of a fully-depleted device, and this bandwidth further confirms that carriers are extracted via drift in these devices on the sub-microsecond timescale.

4. Photoconductor mechanisms and performance

Photoconductors (Fig. 1b) conduct a single carrier type, and so are unipolar, while photodiodes extract carriers of each type. Photoconductors' conductance increases for a duration known as the persistence time following illumination. The difference in the light versus the dark conductance indicates the light level. If the persistence time exceeds the transit time of the flowing carrier through the device, many charges worth of current may be integrated for each photon absorbed. The persistence is determined by the electron–hole pair recombination time, and this is prolonged with the aid of traps (Fig. 2 and Refs. [20,23,25,26,28,47,48].). These traps serve both to delay band-to-band recombination, and also to impede the extraction of the trapped carrier, a condition necessary to photoconductive gain. The physical mechanisms underlying photoconduction have been of interest in bulk materials since early in the history of semiconductors [49,50].

The first solution-cast optoelectronic device to outperform its epitaxial counterparts was a photoconductive photodetector reported in 2006 [20]. A key insight leading to this advance was the realization that excess noise could accumulate along the transport path if the interfaces between the nanoparticles making up the semiconductor film were randomly time-varying due to

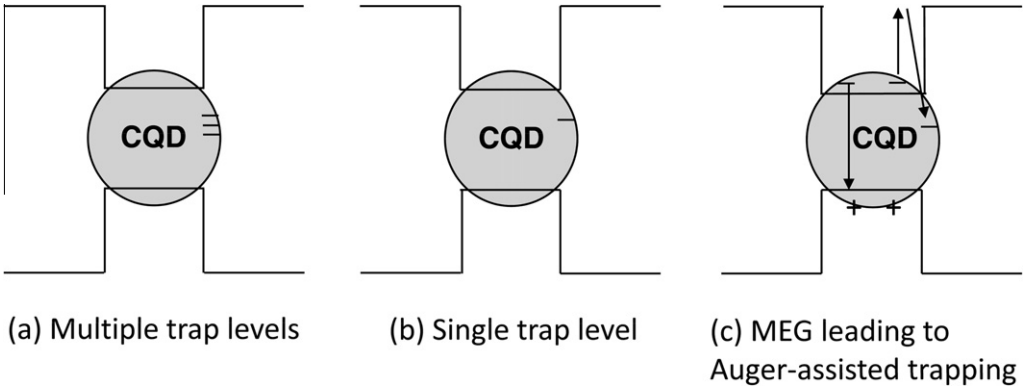

Fig. 2. Trap engineering in photoconductors. Traps extend the lifetime of non-circulating carriers (Fig. 1b), thereby increasing gain. The central light-blue circles represent the colloidal quantum dot. The energy axis is represented in the vertical dimension, the spatial dimension via horizontal axes. The valence band edge spatial profile is the lower solid line, the conduction band edge spatial profile the upper solid line. (a) Multiple sensitizing agents – such as native sulfides, sulfates, and sulfoxides on nanoparticle surfaces – generally result in multiple trap state lifetimes and a multi-time-constant temporal response [20]. In general photodetectors and image sensors require a single time constant to achieve a signal-level-independent bandwidth and substantially linear response. (b) Traps on nanoparticle surfaces of a single chemical species, and thus a single lifetime, have been implemented via advances in process engineering. A single class of chemical species, such as sulfites, produces a single temporal component in the photodetector's response., These photodetectors offer speeds of response compatible with video-frame-rate imaging [25,26]. (c) Multi-exciton generation (MEG), leading to enhanced Auger recombination in quantum dots in the simultaneous presence of at least two excitons, enhances the rate of capture to traps in one recent report [28].

trapping and de-trapping effects from thermally- or optically-generated carriers [51]. Such random events are responsible for the observation of excessive low-frequency noise exhibiting $1/f$ behavior and with time constants associated with the timescales of these spontaneous fluctuations of the barriers. This multiplicative noise, also known as transport noise, was obviated through a processing strategy wherein pure (trap-free) colloidal quantum dot films were first realized; and only once the electrical connections between adjacent nanoparticles were forged were the remaining exposed surfaces of the nanoparticles decorated with sensitizing centers (Fig. 2a). In this way, the modulation of carrier transport along the conduction path by fluctuating barriers was significantly suppressed [52].

Many advances in solution-cast photoconductor performance have since been reported. For example, PbS nanoparticles with a diameter of less than 3 nm can have a bandgap that is three times that of bulk PbS, and the resulting strong quantum confinement can be exploited to achieve high-detectivity visible-wavelength light sensing [21]. The quantum size effect affords wide spectral tunability within a single materials system and processing architecture, enabling multispectral detectors that monolithically integrate pixels sensitive in the visible, near-infrared, and short-wavelength infrared.

Building on a long history of studies of bulk PbS photoconduction [53], recent reports have elucidated the chemical origins of traps having different energies, and different lifetimes, as a function of chemical species and nanoparticle size and preparation. This enabled the implementation of a single trap state lifetime and video-frame-rate-compatible photoconductor behavior [25]. The latter in combination with the abundance of surface traps stemming from the high surface to volume ratio offered by the nanostructured materials has led to dynamic range on the order of 150 dB [21] (defined as 20 $\log(I_{sat}/NEI)$, where I_{sat} is the intensity at which photocurrent saturation onsets and NEI is the minimum detectable intensity or noise-equivalent intensity), well exceeding the requirements of the most demanding imaging applications.

5. Carrier multiplication and prospects

Conventionally, both photodiodes and photoconductors seek to produce a maximum of signal following the generation of at most one electron–hole pair per photon. A further, multiplicative, path to enhanced signal generation arises if numerous photocarriers can be generated for every photon. Carrier multiplication, known in the colloidal quantum dot literature as multi-exciton generation (MEG) [54], offers this possibility. Carrier multiplication has previously been observed in bulk photodetectors [55], and MEG has been observed in colloidal quantum dots for over half a decade [11]; however, its benefits were only recently observed in the photocurrent of an operating colloidal quantum dot device [28,56,57]. Further, the energetic threshold and yield have MEG have been the subject of debate, with variations arising as a function of spectroscopic technique and sample preparation [58–60]. Recently, a photoconductive photodetector employing colloidal quantum dots [28] was observed to exhibit spectrally-invariant internal photoconductive gain until the onset of MEG at a photon energy equal to slightly less than three times the quantum-confined bandgap; at higher photon energies, a steep rise in internal gain was observed. Such phenomena had previously been sought, but not seen, in photodiodes based on similar quantum dot materials [42]. While the Auger recombination process in the presence of multiple excitons rapidly leads to annihilation of primary photoexcitations in photodiodes, the same process leads to efficient ionization [58] and capture to the traps that sensitize photoconductors [61]. Direct ionization of excited photocarriers prior to MEG could in principle also be expected to occur; however, a series of control experiments [28] investigating the size effect and trap-depth-dependence of the internal gain spectrum suggest that direct ionization does not play a leading role in photoresponse. Taken in combination, these findings indicate that the carrier multiplication process occurs more rapidly than both intersubband relaxation and direct capture of excited photocarriers to traps.

6. Conclusions

Solution-processed light sensors offer a wide suite of advantages in imaging and photodetection. The convenient integration of light sensing materials with a variety of substrates enables separate optimization of each function: silicon electronics, ideally suited to volume manufacture, low-noise read-out, and a comprehensive array of analog and digital functions, can be augmented with a 100%-fill-factor, spectrally-tunable, optically dense, low-crosstalk light sensing layer customized for efficient conversion from the optical to the electronic domain. Ever-growing dexterity

in manipulating materials at the nanoscale – the engineering matter on the quantum and plasmonic lengthscales – provides for an unheralded degree of customization and optimization in coming generations of light sensing arrays.

Acknowledgements

This publication is based in part on work supported by Award No. KUS-11-009-21, made by King Abdullah University of Science and Technology (KAUST). We also acknowledge the Natural Sciences and Engineering Research Council of Canada (NSERC I2I Programme), the Ontario Centers of Excellence; the Canada Foundation for Innovation and Ontario Innovation Trust; and the Canada Research Chairs.

References

[1] L. Sosnowski et al., Lead sulphide photoconductive cells, Nature 159 (1947) 818–819.
[2] S. Espevik et al., Mechanism of photoconductivity in chemically deposited lead sulfide layers, Journal of Applied Physics 42 (1971) 3513–3529.
[3] T. Kanno et al., Uncooled infrared focal plane array having 128×128 thermopile detector elements, Proceedings of SPIE - The International Society for Optical Engineering 2269 (1994) 450–459.
[4] I. Nausieda et al., An organic active-matrix imager, IEEE Transactions on Electron Devices 55 (2008) 527–532.
[5] V.A. Shchukin, D. Bimberg, Spontaneous ordering of nanostructures on crystal surfaces, Reviews of Modern Physics 71 (1999) 1125–1171.
[6] C.B. Murray et al., Synthesis and characterization of nearly monodisperse CdE (E = S, Se, Te) semiconductor nanocrystallites, Journal of the American Chemical Society 115 (1993) 8706–8715.
[7] L. Brus, Electronic wave functions in semiconductor clusters: experiment and theory, Journal of Physical Chemistry 90 (1986) 2555–2560.
[8] D.V. Talapin, C.B. Murray, Applied physics: PbSe nanocrystal solids for n- and p-channel thin film field-effect transistors, Science 310 (2005) 86–89.
[9] D. Yu et al., Variable range hopping conduction in semiconductor nanocrystal solids, Physical Review Letters 92 (2004) 216802-1.
[10] A. Pandey, P. Guyot-Sionnest, Slow electron cooling in colloidal quantum dots, Science 322 (2008) 929–932.
[11] R.D. Schaller, V.I. Klimov, High efficiency carrier multiplication in PbSe nanocrystals: implications for solar energy conversion, Physical Review Letters 92 (2004) 186601–186603.
[12] V.I. Klimov et al., Optical gain and stimulated emission in nanocrystal quantum dots, Science 290 (2000) 314–317.
[13] V.I. Klimov et al., Quantization of multiparticle Auger rates in semiconductor quantum dots, Science 287 (2000) 1011–1014.
[14] V.I. Klimov, Optical nonlinearities and ultrafast carrier dynamics in semiconductor nanocrystals, Journal of Physical Chemistry B 104 (2000) 6112–6123.
[15] R.J. Ellingson et al., Highly efficient multiple exciton generation in colloidal PbSe and PbS quantum dots, Nano Letters 5 (2005) 865–871.
[16] G. Yu et al., Semiconducting polymer diodes: large size, low cost photodetectors with excellent visible-ultraviolet sensitivity, Applied Physics Letters 64 (1994) 3422–3424.
[17] N.C. Greenham et al., Charge separation and transport in conjugated-polymer/semiconductor-nanocrystal composites studied by photoluminescence quenching and photoconductivity, Physical Review B – Condensed Matter and Materials Physics 54 (1996) 17628–17637.
[18] P. Peumans et al., Efficient, high-bandwidth organic multilayer photodetectors, Applied Physics Letters 76 (2000) 3855–3857.
[19] D.C. Oertel et al., Photodetectors based on treated CdSe quantum-dot films, Applied Physics Letters 87 (2005) 213505-1–213505-3.
[20] G. Konstantatos et al., Ultrasensitive solution-cast quantum dot photodetectors, Nature 442 (2006) 180–183.
[21] G. Konstantatos et al., Sensitive solution-processed visible-wavelength photodetectors, Nature Photonics 1 (2007) 531–534.
[22] M. Boberl et al., Inkjet-printed nanocrystal photodetectors operating up to 3 μm wavelengths, Advanced Materials 19 (2007) 3574–3578.
[23] H.Y. Chen et al., Nanoparticle-assisted high photoconductive gain in composites of polymer and fullerene, Nature Nanotechnology 3 (2008) 543–547.
[24] S. Hinds et al., Smooth-morphology ultrasensitive solution-processed photodetectors, Advanced Materials 20 (2008) 4398–4402.
[25] G. Konstantatos et al., Engineering the temporal response of photoconductive photodetectors via selective introduction of surface trap states, Nano Letters 8 (2008) 1446–1450.
[26] G. Konstantatos et al., Sensitive solution-processed Bi_2S_3 nanocrystalline photodetectors, Nano Letters 8 (2008) 4002–4006.
[27] Y. Jin et al., Solution-processed ultraviolet photodetectors based on colloidal ZnO nanoparticles, Nano Letters 8 (2008) 1649–1653.
[28] V. Sukhovatkin et al., Colloidal quantum-dot photodetectors exploiting multiexciton generation, Science 324 (2009) 1542–1544.
[29] J.P. Clifford et al., Fast, sensitive and spectrally tuneable colloidal-quantum-dot photodetectors, Nature Nanotechnology 4 (2009) 40–44.
[30] T. Rauch et al., Near-infrared imaging with quantum-dot-sensitized organic photodiodes, Nature Photonics 3 (2009) 332–336.
[31] X. Gong et al., High-detectivity polymer photodetectors with spectral response from 300 nm to 1450 nm, Science 325 (2009) 1665–1667.
[32] A. Pourret et al., Atomic layer deposition of ZnO in quantum dot thin films, Advanced Materials 1 (2009) 232–235.
[33] R.L. Petritz, Theory of photoconductivity in semiconductor films, Physical Review 104 (1956) 1508–1516.
[34] S. Cova et al., Avalanche photodiodes and quenching circuits for single-photon detection, Applied Optics 35 (1996) 1956–1976.
[35] J. Piotrowski, W. Gawron, Ultimate performance of infrared photodetectors and figure of merit of detector material, Infrared Physics and Technology 38 (1997) 63–68.
[36] K.W. Johnston et al., Efficient schottky-quantum-dot photovoltaics: the roles of depletion, drift, and diffusion, Applied Physics Letters 92 (2008) 122111–122113.
[37] S.W. Clark et al., Resonant energy transfer in PbS quantum dots, Journal of Physical Chemistry C 111 (2007) 7302–7305.
[38] E.J.D. Klem et al., Efficient solution-processed infrared photovoltaic cells: planarized all-inorganic bulk heterojunction devices via inter-quantum-dot bridging during growth from solution, Applied Physics Letters 90 (2007) 183113–183115.
[39] K.W. Johnston et al., Schottky-quantum dot photovoltaics for efficient infrared power conversion, Applied Physics Letters 92 (2008) 151115–151118.
[40] G.I. Koleilat et al., Efficient, stable infrared photovoltaics based on solution-cast colloidal quantum dots, ACS Nano 2 (2008) 833–840.
[41] J.M. Luther et al., Schottky solar cells based on colloidal nanocrystal films, Nano Letters 8 (2008) 3488–3492.
[42] M. Law et al., Determining the internal quantum efficiency of PbSe nanocrystal solar cells with the aid of an optical model, Nano Letters 8 (2008) 3904–3910.
[43] W. Ma et al., Photovoltaic devices employing ternary PbS_xSe_{1-x} nanocrystals, Nano Letters 9 (2009) 1699–1703.
[44] D.A.R. Barkhouse et al., Thiols passivate recombination centers in colloidal quantum dots leading to enhanced photovoltaic device efficiency, ACS Nano 2 (2008) 2356–2362.
[45] K.M. Coakley, M.D. McGehee, Conjugated polymer photovoltaic cells, Chemistry of Materials 16 (2004) 4533–4542.
[46] M. Ettenberg, A little night vision, Advanced Imaging 20 (2005) 29–32.
[47] S.A. McDonald et al., Solution-processed PbS quantum dot infrared photodetectors and photovoltaics, Nature Materials 4 (2005) 138–142.
[48] T.P. Osedach et al., Lateral heterojunction photodetector consisting of molecular organic and colloidal quantum dot thin films, Applied Physics Letters 94 (2009) 043307–043309.
[49] R. Bube, Photoconductivity of solids, Wiley, New York, 1960.
[50] A. Rose, Concepts in Photoconductivity and Allied Problems, Wiley, New York, 1963.
[51] A. Carbone, P. MAzzetti, Grain-boundary effects on photocurrent fluctuations in polycrystalline photoconductors, Physical Review B 57 (1998) 2454–2460.
[52] A. Carbone, P. MAzzetti, F. Rossi, Low-frequency photocurrent noise in semiconductors: effect of nonlinear current–voltage characteristics, Applied Physics Letters 78 (2001) 2518–2520.
[53] G.W. Mahlman, Photoconductivity of lead sulfide films, Physical Review 103 (1956) 1619–1630.
[54] A.J. Nozik, Multiple exciton generation in semiconductor quantum dots, Chemical Physics Letters 457 (2008) 3–11.
[55] A. Smith, D. Dutton, Behavior of lead sulfide photocells in the ultraviolet, Journal of the Optical Society of America A: Optics and Image Science 48 (1958) 1007–1009.
[56] S.J. Kim et al., Multiple exciton generation and electrical extraction from a PbSe quantum dot photoconductor, Applied Physics Letters 92 (2008) 031107.
[57] S.J. Kim et al., Carrier multiplication in a PbSe nanocrystal and P3HT/PCBM tandem cell, Applied Physics Letters 92 (2008) 191107.
[58] J.A. McGuire et al., New aspects of carrier multiplication in semiconductor nanocrystals, Accounts of Chemical Research 41 (2008) 1810–1819.
[59] G. Nair et al., Carrier multiplication yields in PbS and PbSe nanocrystals measured by transient photoluminescence, Physical Review B 78 (2008) 125325.
[60] J.J.H. Pijpers et al., Assessment of carrier-multiplication efficiency in bulk PbSe and PbS, Nature Physics 5 (2009) 811–814.
[61] A.J. Nozik, Nanophotonics: making the most of photons, Nature Nanotechnology 4 (2009) 548–549.